ACS APPLIED ENERGY MATERIALS

Article

Cite This: ACS Appl. Energy Mater. 2020, 3, 861−867

www.acsaem.org

PEDOT Thin Films with n-Type Thermopower

José F. Serrano-Claumarchirant,[†] Mario Culebras,[§] Rafael Muñoz-Espí,[†] Andrés Cantarero,[‡] Clara M. Gómez,[†] and Maurice N. Collins*[,§]

[†]Institute of Materials Science (ICMUV) and [‡]Institute for Molecular Sciences (ICMol), Universitat de València, c/Catedràtic Jose′ Beltra′n 2, 46980 Paterna, Spain

[§]School of Engineering, Stokes Laboratories, Bernal Institute, University of Limerick, V94T9PX Limerick, Ireland

Supporting Information

ABSTRACT: The synthesis of n-type organic semiconductors is challenging as reduced states are difficult to obtain due to their instability in air. Here, we report tailoring of semiconducting behavior through control of surfactant concentration during synthesis of poly(3,4-ethylenedioxythiophene) (PEDOT) nanoparticles. Nanoparticles were synthesized by miniemulsion polymerization, where stable suspensions were used to produce polymer films by a simple casting technique on poly(ethylene terephthalate) (PET) substrates. The electrical conductivity and Seebeck coefficients were measured as a function of surfactant concentration. It was found that conductivity decreases 3 orders of magnitude as surfactant concentration increased, and remarkably the Seebeck coefficient switched from p-type to n-type. To further elucidate this finding, doping effects were studied by Raman, ultraviolet−visible (UV−vis), and electron spin resonance (EPR) spectroscopies. Finally, a thermoelectric module was developed by using the n-type PEDOT synthesized in this work and a standard p-type PEDOT:PSS.

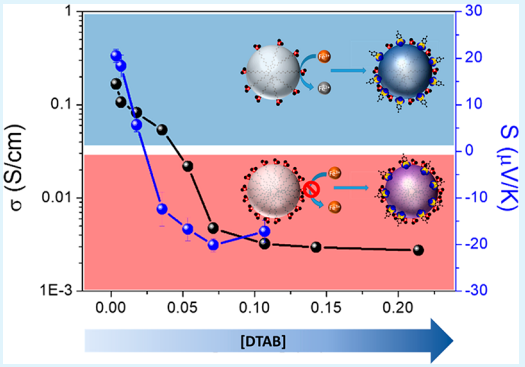

KEYWORDS: *PEDOT nanoparticles, thin film, electrical conductivity, Seebeck coefficient, n-type organic semiconductors*

INTRODUCTION

To build a thermoelectric device, both n-type and p-type materials are required. However, n-type doping is especially complex in organic semiconductors. Doping mechanisms involve reduction states that are not stable in air.[1−3] Therefore, there is currently major scientific interest in the search for a stable n-type conducting polymer for the manufacture of thermoelectric modules.[2] Intrinsically conducting polymers (ICPs) are attracting widespread attention due to their promise in organic light-emitting diodes (OLEDs),[4,5] organic solar cells (OSC),[6,7] supercapacitors,[8−11] and thermoelectric devices.[12,13] They exhibit several desirable properties, including flexibility, low cost, ease of chemical modification, and flexible processing, which render them a viable alternative to inorganic semiconductors.[14−16] Thin ICP films are being used as coatings also for corrosion protection[17] as well as electromagnetic shields,[18] radar absorbers,[19] sensors,[20,21] and polymeric actuators.[22] There has been an ever increasing number of scientific studies dedicated to these topics in recent years.[23]

Conducting polymers transfer electrons via conjugated π-bonds along their chains. Electrons may be added (n-doping) or removed (p-doping) from the polymer chain, creating free carriers called polarons and/or bipolarons.[24] Controlling the doping level through the use of reductants[25,26] or by electrochemical dedoping[27] is critical to maximize the performance of thermoelectric materials. The thermoelectric efficiency is expressed in terms of the dimensionless figure of merit (ZT), where $ZT = \sigma S^2 T/\kappa$, σ is the electrical conductivity, T is the absolute temperature, S is the Seebeck coefficient, and κ is the thermal conductivity. The maximum thermoelectric efficiency is obtained when doping levels are optimized to produce the maximum power factor ($= S^2\sigma$) and the minimum thermal conductivity. Generally, electrical conductivity increases when the Seebeck coefficient decreases,[13,25,2721,22] while it is known that nanostructuration of a material improves the Seebeck coefficient by phonon scattering which reduces thermal conductivity.[24,28,29]

Conducting polymers are produced via electrochemical polymerization, photopolymerization by irradiating the precursor, and chemical polymerization of the monomer in the presence of an oxidizing agent,[1623] while miniemulsion polymerization is utilized to obtain polymer nanoparticles within stable water suspensions[30] and allows ease of functionalization of the nanoparticle surface during synthesis.[31,32] In addition, it is possible to dope the conductive polymer with oxidants, such as iron(III) *p*-toluenesulfonate, ammonium persulfate, and iron(III) oxide.[33] Furthermore, suspensions of conducting polymer nanoparticles can be used for the preparation of thin film coatings by techniques such as

Received: October 8, 2019
Accepted: December 17, 2019
Published: December 17, 2019

DOI: 10.1021/acsaem.9b01985
ACS Appl. Energy Mater. 2020, 3, 861−867

Table 1. Reactants Used To Study DTAB Influence on PEDOT Polymerization with Molar Ratio EDOT:FeTos of 1:1

reactants	amounts								
DTAB (M)	0.0035	0.0071	0.0178	0.0357	0.05354	0.0714	0.1071	0.1428	0.2141
EDOT (mL)	0.2	0.2	0.2	0.2	0.2	0.2	0.2	0.2	0.2
Fe-Tos (M)	2.8×10^{-2}	2.8×10^{-2}	2.8×10^{-2}	2.8×10^{-2}	2.8×10^{-2}	2.8×10^{-2}	2.8×10^{-2}	2.8×10^{-2}	2.8×10^{-2}

drop-casting, spin-coating, and layer-by-layer dip-coating for several high-end applications,[16] including electrodes in supercapacitors, batteries,[34] and solar cells.[35]

Up to now, only p-type conducting polymers have exhibited good thermoelectric performance due to their high conductivity (over 1000 S/cm) and high stability with a ZT around 0.2−0.4.[36,13,26] For n-type conducting polymers the situation in terms of thermoelectric efficiency is completely different. Factors such as low n-doping efficiency which restricts the charge carrier density, low charge carrier mobilities after doping, which directly limit intra- and interchain charge transport and poor air stabilities, decrease their electrical conductivity and therefore their thermoelectric efficiency.[37] Only a few polymers such as poly{*N*,*N*′-bis(2-octyldodecyl)-1,4,5,8-naphthalenedicarboximide-2,6-diyl]-*alt*-5,5′-(2,2′-bithiophene) (P(NDIOD-T2) doped by dihydro-1*H*-benzimidazol-2-yl (N-DBI) derivatives (PF 0.6 μW/(m K^2)),[38] or BDPPV, ClBDPPV, and FBDPPV doped with N-DMBI[39] (PF up to 28 μW/(m K^2)) highlight over the rest in terms of thermoelectric performance. For n-type polymer nanocomposites the situation is more promising with PFs around 200 μW/(m K^2) for polyethylenimine (PEI)/CNTs, the predominant material.[40,41,36]

Here, we show for the first time an n-type behavior in PEDOT films prepared from nanoparticles. Semiconducting can be easily switched from p- to n-type by tailoring surfactant concentrations. These nanoparticle suspensions are stable for several months.

MATERIALS AND METHODS

Materials. PEDOT:PSS (conductive grade) 3,4-ethylenedioxythiophene (EDOT, 97%), iron(III) *p*-toluenesulfonate hexahydrate (FeTos, 98%), and dodecyltrimethylammonium bromide (DTAB, 98%) were purchased from Sigma-Aldrich and used as received.

Synthesis of PEDOT Nanoparticles and Films. Synthesis was performed via chemical oxidation polymerization in a miniemulsion using a cationic surfactant (DTAB). Table 1 summarizes reactants and compositions used. DTAB was dissolved in 40 mL of ultrapure water. Then, 0.2 mL of EDOT was added to the cationic surfactant solution, and the mixture was magnetically stirred for 10 min. The mixture was then sonicated using a Branson 450-D sonifier with 70% of amplitude in pulsed mode (90% of the nominal power of the equipment, 1/2 in. tip) for 5 min, while cooled in an ice−water bath. After this process, a white miniemulsion was obtained. This miniemulsion was transferred to a reaction flask and placed in an oil bath thermostated at 45 °C. Finally, 25 mL of FeTos solution was added to the reaction flask, leaving the polymerization to proceed for 24 h under constant stirring.

The obtained PEDOT nanoparticles were purified by centrifugation at 8000 rpm for 20 min. The resulting powder was redispersed in 40 mL of ultrapure water as follows: the nanoparticle dispersion was sonicated for 30 min in an ultrasound bath, then 20 min in a Branson 450-D sonifier (70% of the nominal power of the equipment, 1/2 in. tip), and finally 20 min in an ultrasound bath again.

The influence of DTAB concentration was studied by variation from 0.0035 to 0.214 M (see experimental details in Table 1).

After obtaining a stable PEDOT suspension, thin films were prepared by a simple casting method (see Figure 1). First, PET

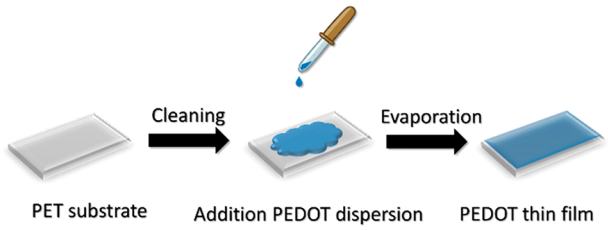

Figure 1. Scheme of thin film preparation by casting.

substrates were bath-sonicated in ethanol for 5 min, then dried at 60 °C overnight, and cooled to room temperature. Subsequently, the PEDOT dispersion was cast onto PET substrates. After water evaporation at 25 °C under vacuum overnight, homogeneous thin films of about 2 μm thick were obtained (see Table S2).

Thermoelectric Module Manufacture. The thermoelectric device was produced by using PEDOT:PSS and PEDOT:DTAB synthesized with optimized levels of of DTAB (0.035 M). Five strips of each polymer were cast as described previously. The resulting polymer strips were electrically connected by using silver paste.

Characterization. Transmission electron microscopy (TEM) (JEOL JEM-1010) operating at 100 kV equipped with a digital camera (MegaView III). The particle size was statistically analyzed from TEM images by measuring a minimum of 100 particles utilizing ImageJ software.[42] Scanning electron microscopy (SEM) images were captured with a HITACHI S-4800 microscope operated at 1 kV.

We determined the electrical conductivity (σ) with a custom-built device using the van der Pauw method; four contacts were used to eliminate the effect of contact resistance. A Keithley 2400 power supply was used as a power source. Two resistance values, R_1 and R_2, were measured by introducing current between two lateral contacts and measuring the voltage in the parallel contacts located at the other side of the sample. The conductivity can be measured by solving the van der Pauw equation:[43]

$$e^{-\pi d\sigma R_1} + e^{-\pi d\sigma R_2} = 1 \quad (1)$$

where d is the sample thickness (measured by using a Veeco Dektak stylus profilometer).

For the Seebeck effect measurements, a second custom built device was utilized. The experimental setup consisted of two copper blocks: one heated by resistance heating and the other cooled by water. The sample is placed between these two blocks. A linear temperature gradient is created along the sample and the resulting voltage at the two ends is recorded. Measurements were performed at room temperature applying a ΔT of 10 K. The Seebeck coefficient is determined to be the ratio between the electrical potential, ΔV, and the temperature difference, ΔT, as follows:

$$S = \frac{\Delta V}{\Delta T} \quad (2)$$

The temperatures at the ends of the sample are controlled by means of a Lakeshore 340 temperature controller using calibrated PT100 resistors. The temperatures were varied to check the linearity of the Seebeck coefficient (S is the slope of $V(T)$). To record the electric potential, a Keithley 2750 multimeter switching system was employed. Both instruments were coupled by using Labview software.

The film thickness was measured with an optical profilometer (Dektak 150). Reported values are an average of at least five measurements per film. Raman scattering measurements were performed at room temperature in backscattering configuration using a Jobin Yvon T64000 spectrometer equipped with a liquid-

DOI: 10.1021/acsaem.9b01985
ACS Appl. Energy Mater. 2020, 3, 861−867

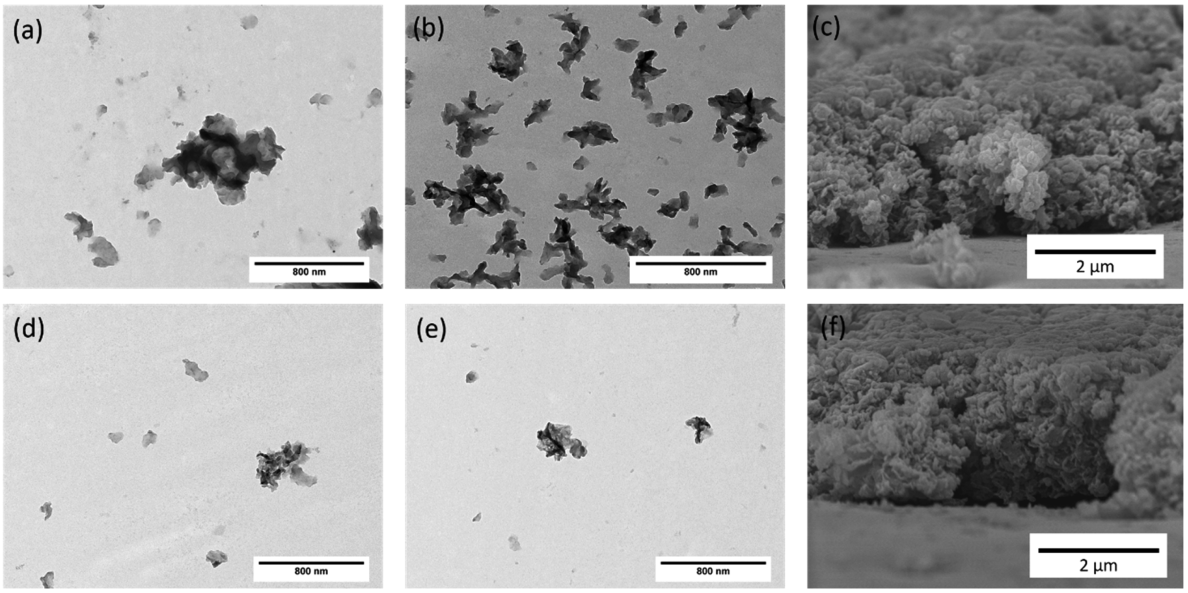

Figure 2. TEM images of PEDOT nanoparticles with a molar ratio EDOT:FeTos 1:1 by using (a) 0.0035, (b) 0.035, (d) 0.071, and (e) 0.214 M DTAB. SEM cross section of PEDOT nanoparticles thin films: (c) 0.0035 and (f) 0.035 M.

nitrogen-cooled open electrode charge-coupled device (OECCD camera). The excitation line of 514.53 nm was provided by an Ar/Kr laser focused on the sample using a 100× microscope objective with a numerical aperture (NA) = 0.90 (Olympus). This setup focuses the light on an area of around 10 μm on the sample. Special care was taken to avoid sample heating during experiments, with power down to a few microwatts in the total area. Ultraviolet−visible spectroscopy measurements were performed with a Shimadzu UV-2501PC spectrophotometer covering the range from 1000 to 300 nm utilizing quartz cells. EPR spectroscopy (Model Bruker ELEXYS E580) was measured in thin films at room temperature by using the pulsed X-band.

RESULTS AND DISCUSSION

The morphology of PEDOT nanoparticles obtained by miniemulsion polymerization were studied by TEM. All nanoparticles presented flaked morphology, regardless of the amount of DTAB employed during the synthesis. This observation can be explained by the fact that during polymerization Fe^{3+} ions surround the EDOT droplets, which are subsequently stabilized by DTAB. The electrostatic repulsion between the positive charge from DTAB and Fe^{3+} ions leads to a decrease in the polymerization rate of EDOT, and therefore irregular nanoparticle morphologies occur. Additional TEM images are shown in the Supporting Information (see Figure S1) for PEDOT nanoparticles obtained from the synthesis using DTAB as surfactant with molar ratio EDOT:FeTos 1:2. In this case, the aggregation level is higher compared to the nanoparticles obtained at molar ratio 1:1 because the oxidant content is higher. All nanoparticle suspensions were stable. However, suspensions prepared at a DTAB concentration of 0.0035 M display instabilities after a couple of days, after the redispersion process, while all the other dispersions were stable for long periods of time (weeks).

To evaluate the potential application of these PEDOT nanoparticles in coatings for thermoelectric applications, thin films were prepared by casting suspensions on PET substrates. SEM micrographs of cross sections of representative films prepared from the nanoparticle dispersions are shown in Figure 2c,f.

Electrical conductivity and Seebeck coefficient values are shown in Figure 3 for the molar ratio EDOT:FeTos 1:1

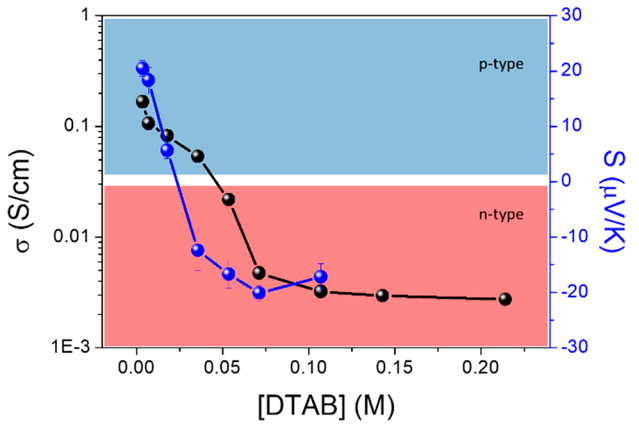

Figure 3. Electrical conductivity and Seebeck coefficient of PEDOT film as a function of DTAB concentration with the molar ratio EDOT:FeTos.

(additional measurements are shown in Figure S3 for the molar ratio EDOT:FeTos 1:2). Electrical conductivity decreases as the DTAB concentration increases. This is presumably due to the DTAB stabilization of the EDOT droplet in the miniemulsion; therefore, this droplet carries a positive charge due to the presence of the surfactant (DTAB) at the interface. As the oxidant (Fe^{3+}) is also positively charged, there is an electrostatic repulsion between the surfactant and oxidant, and this inhibits the Fe^{3+} interaction with the EDOT droplets, with the consequence that the oxidation polymerization is inhibited and finally terminated as the DTAB concentration increases (see Figure 4).

The Seebeck coefficient of these materials is unusual. For example, for PEDOT nanoparticles at molar ratio EDOT:FeTos 1:1, the Seebeck coefficient is positive, 22 mV/K, at a DTAB concentration of 0.0035 M. However, when the concentration of DTAB increases to 0.035 M, the Seebeck

DOI: 10.1021/acsaem.9b01985
ACS Appl. Energy Mater. 2020, 3, 861−867

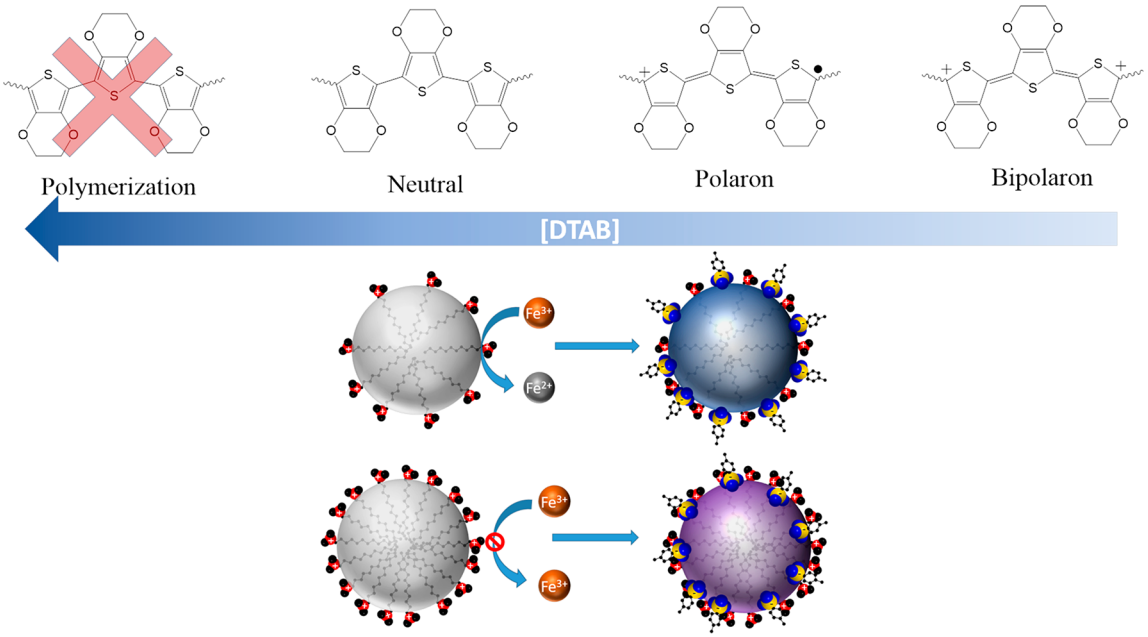

Figure 4. Schematic of doping evolution of PEDOT as a function of DTAB concentration.

coefficient switches to negative values, indicating a strong change in the semiconducting behavior to an n-type semiconductor, as shown in Figure 3. As the surfactant concentration increases further, the Seebeck coefficient decreases to low values. A similar trend was observed for the case of PEDOT nanoparticles at the molar ratio EDOT:FeTos 1:2 (see Figure S2).

The Seebeck coefficient was ~20 μV/K at a surfactant concentration of 0.0035 M, a typical value for highly doped PEDOT.[22,33] However, at a higher surfactant concentration of 0.035 M, the switch occurs to n-type behavior with a Seebeck coefficient of −12 μV/K. When the concentration of surfactant reaches 0.071 M, the highest n-type Seebeck coefficient of approximately −21 μV/K is achieved. At higher surfactant concentrations (0.1 M) the Seebeck coefficient decreases due to the inhibition of EDOT polymerization which results in a decay of both electrical conductivity and Seebeck coefficient. It is possible to estimate the *ZT* range by using thermal conductivity values from PEDOT measurements in other report (0.2−1.0 W/(m K)).[44] Thus, the *ZT* range could be between 2×10^{-6} and 1.04×10^{-5} for p-type and between 1.75×10^{-7} and 9×10^{-7} for n-type nanoparticles.

In previous work, we have reported a similar procedure to synthesize PEDOT nanoparticles with p-type behavior using Lutensol AT50 as a surfactant.[33] The reaction conditions were the same, but n-type behavior was not observed. Normally for oxidation polymerization of PEDOT electrons are removed from the polymer generating holes. The n-type behavior in these materials may be explained by the stabilization of an intermediate oxidation state which promotes n-type conduction rather than p-type.

Figure 5 shows the Raman spectra of films prepared from PEDOT nanoparticles synthesized with a molar ratio of EDOT:FeTos 1:1. The Raman intensity between the samples is very similar, indicating a higher presence of neutrally charged p-bonds in comparison to the oxidized state of the conjugated π-system (polarons and bipolarons) typical for medium doped PEDOT. Interestingly, the sample with 0.071 M DTAB surfactant presents a lower intensity than the other samples

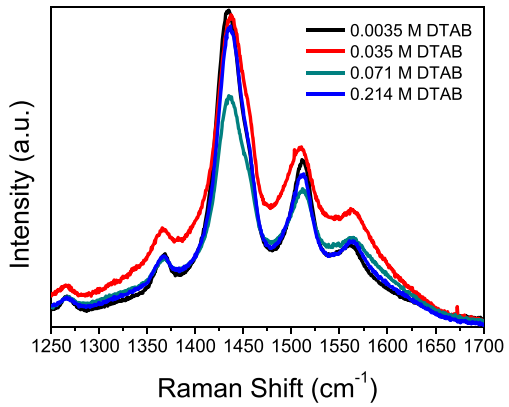

Figure 5. Raman spectra of PEDOT film as a function of DTAB concentration with the molar ratio EDOT:FeTos 1:1.

due to an electronic alteration in the p-bond conjugated system. This electronic alteration is attributed to a higher ratio of polaronic states/neutral p-bonds compared to the nanoparticles synthesized with 0.0035 and 0.035 M surfactant where the conjugated π-system is longer due to higher degrees of polymerization. In other words, although the oxidation power is higher at lower surfactant concentrations, so is the polymerization degree; therefore, a greater length of conjugated π-bonds chains is present. However, at 0.071 M surfactant the polymerization degree is decreased (shorter chain of π-bonds), but the oxidation power is now capable of producing polarons changing the oxidation state and increasing the ratio of polaronic states in comparison to neutral p-bonds. For high concentrations of surfactant (0.2 M) the oxidation degree is not strong enough to produce doped states (only conjugated p-bonds are present); therefore, the Raman intensity increases.

For samples with a molar ratio 1:2 as shown in Figure S4, results follow the same trend. However, the particles synthesized at 0.0035 M surfactant present the lowest Raman

DOI: 10.1021/acsaem.9b01985
ACS Appl. Energy Mater. 2020, 3, 861−867

intensity, indicating high doping levels of PEDOT. This is due to the increased iron content in the solution.

Figures 6 shows the UV−vis spectra of PEDOT nanoparticles synthesized with the molar ratio EDOT:FeTos 1:1.

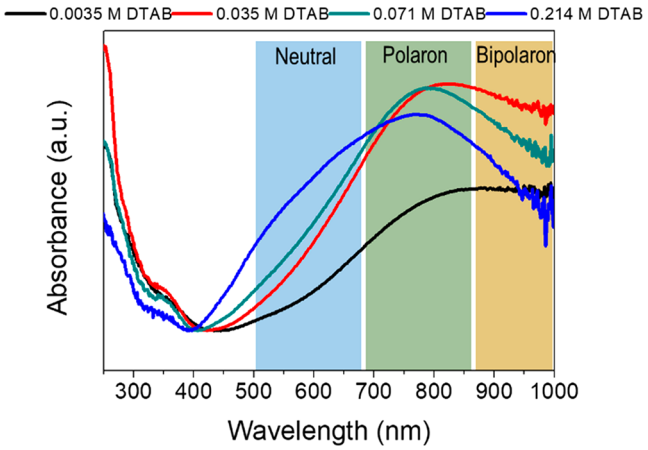

Figure 6. UV−vis spectra of PEDOT film as a function of DTAB concentration with the molar ratio EDOT:FeTos 1:1.

The PEDOT nanoparticles synthesized with 0.214 M surfactant show higher absorption in the region between 500 and 600 nm, corresponding to the electronic transition of the electrons in the neutral p-bonds, and they exhibit low doping levels compared with the remaining samples.

For the lowest concentration of surfactant (0.0035 M) the maximum absorption is located in the range of 800−1000 nm, which is characteristic for bipolaronic states, indicating that these states are the predominant oxidation form and are responsible for electric transport in PEDOT chains. For samples that show n-type behavior (0.035 and 0.071 M) the maximum absorption is shifted to lower wavelengths, 820 and 780 nm for the PEDOT nanoparticles prepared using 0.035 and 0.071 M surfactant, respectively. Results suggest that the predominant oxidation state are polarons, and this agrees with recent studies on absorption spectroscopy of polaronic and bipolaronic states of PEDOT.[45] Thus, there is clear relationship between the surfactant concentration and the doping level of the PEDOT nanoparticles. In addition, the energy levels of the HOMO and LUMO orbitals (estimated by cyclic voltammetry measurements[46−48]) are affected as shown in Figure S7c. Overall, there is a clear relationship between the polaronic states and the n-type behavior observed in the Seebeck coefficient measurements.

Figure 7 shows electron paramagnetic resonance (EPR) results for PEDOT films (molar ratio EDOT:FeTos 1:1). The decrease of the EPR signal at surfactant concentrations of 0.0035 M is attributed to the presence of bipolarons, double charge carriers with zero spin that are not detectable by EPR.[49,50] PEDOT nanoparticles in this state display maximum values for electrical conductivity (see Figure 3). For 1:1 molar ratios of EDOT:FeTos at 0.035 M surfactant, the EPR signal increases, indicating a change from bipolaron to polaron conduction with a corresponding reduction in electrical conductivity. A similar trend has been observed for 1:2 molar ratio EDOT:FeTos as shown in Figure S6. The EPR signal increases for samples prepared with 0.035 and 0.071 M surfactant due to the transition from bipolaron to polaron conduction which follows the pattern as explained above.

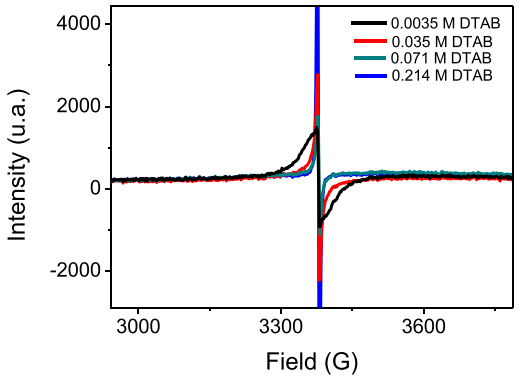

Figure 7. EPR spectra of PEDOT films as a function of DTAB concentration with the molar ratio EDOT:FeTos 1:1.

Figure 8 shows the results of a proof of concept thermoelectric module developed to show the potential of

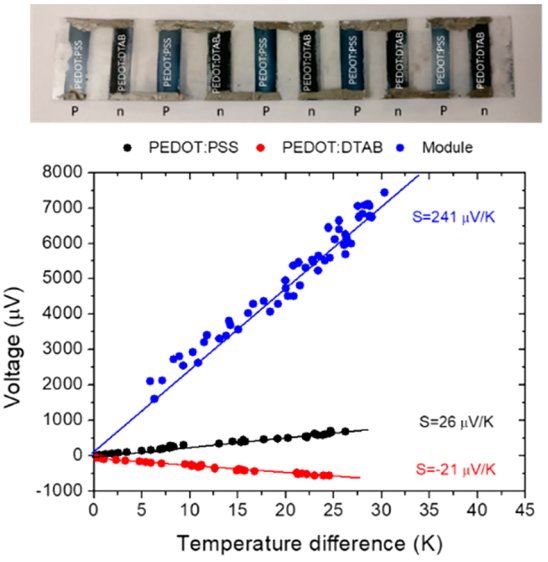

Figure 8. Voltage as a function of the temperature for PEDOT:PSS, PEDOT:DTAB, and TE module.

these materials as n-type conducting polymers for thermoelectric devices. A standard well-established PEDOT:PSS was used as p-type material. The thermoelectric module was built consisting of five PEDOT:PSS strips coupled with five PEDOT:DTAB strips prepared with a molar ratio EDOT/FeTos 1:1 and DTAB concentration of 0.071 M. All the strips were electrically connected. A plot of the voltage as a function of temperature clearly shows an increase by a factor 10 due to the combined thermoelectric effect of the PEDOT strips, with both strips displaying n-type behavior and p-type behavior. This represents strong evidence of the n-type behavior of PEDOT:DTAB nanoparticles. In addition, the values of negative Seebeck coefficient remain in the same order as a function of time for several months which highlights the stability of these materials in air.

CONCLUSIONS

PEDOT nanoparticles have been synthesized by using oxidative polymerization in a miniemulsion in the presence of DTAB as a surfactant. The morphology of the nanoparticles is dependent on the concentration of surfactant and the

DOI: 10.1021/acsaem.9b01985
ACS Appl. Energy Mater. 2020, 3, 861−867

reducing agent FeTos. The electrical conductivity of the subsequently produced films decreases as a function of surfactant concentration, and this is attributed to the positive charge on the surfactant, which is postulated to inhibit the polymerization of PEDOT through electrostatic repulsion of the positively charged oxidant FeTos. In addition, we observe a switch from p- to n-type behavior, which is influenced by the surfactant concentration utilized during synthesis. The n-type behavior in these materials is attributed to the stabilization of an intermediate oxidation state which promotes n-type conduction. This implies that electronic states involved in charge transfer mechanisms can be tailored during synthesis of PEDOT nanoparticles.

■ ASSOCIATED CONTENT

Supporting Information

The Supporting Information is available free of charge at https://pubs.acs.org/doi/10.1021/acsaem.9b01985.

Additional characterization of PEDOT:DTAB nanoparticles synthesized by using the molar ratio EDOT:FeTos 1:2 (PDF)

■ AUTHOR INFORMATION

Corresponding Author

*E-mail: maurice.collins@ul.ie.

ORCID

Mario Culebras: 0000-0001-9244-9347
Rafael Muñoz-Espí: 0000-0002-8146-2332
Andrés Cantarero: 0000-0003-1999-4933
Maurice N. Collins: 0000-0003-2536-4508

Author Contributions

J.F.S.C. performed the experimental work. M.C. built the thermoelectric module. R.M.E. performed the Raman studies. C.G. and A.C. devised the experimental program. M.N.C. analyzed the data.

Notes

The authors declare no competing financial interest.

■ ACKNOWLEDGMENTS

This research was supported by Dirección General de Investigación Científica y Técnica through a grant of the Program Consolider Ingenio (Grant CSD2010-0044) and Grant MAT2015-63955-R. J.F.S.C. acknowledges the financial support by the Spanish Ministry of Education, Culture and Sport through the FPU training program. Finally, R.M.E. thanks the financial support from the Spanish Ministry of Economy and Competitiveness through a Ramón y Cajal grant (Grant RYC-2013-13451).

■ ABBREVIATIONS

EDOT, 3,4-ethylenedioxythiophene; PEDOT, poly(3,4-ethylenedioxythiophene); FeTos, iron(III) *p*-toluenesulfonate hexahydrate; DTAB, dodecyltrimethylammonium bromide; TEM, transmission electron microscopy; SEM, scanning electron microscopy; EPR, electron paramagnetic resonance.

■ REFERENCES

(1) de Leeuw, D. M.; Simenon, M. M. J.; Brown, A. R.; Einerhand, R. E. F. Stability of n-type doped conducting polymers and consequences for polymeric microelectronics devices. *Synth. Met.* **1997**, *87*, 53−59.

(2) Quinn, J. T. E.; Zhu, J.; Li, X.; Wang, J.; Li, Y. Recent progress in the development of n-type organic semiconductors for organic field effect transistors. *J. Mater. Chem. C* **2017**, *5* (34), 8654−8681.

(3) Du, Y.; Chen, J.; Liu, X.; Lu, C.; Xu, J.; Paul, B.; Eklund, P. Flexible n-Type Tungsten Carbide/Polylactic Acid Thermoelectric Composites Fabricated by Additive Manufacturing. *Coatings* **2018**, *8* (1), 25.

(4) Burroughes, J. H.; Bradley, D. D. C.; Brown, A. R.; Marks, R. N.; Mackay, K.; Friend, R. H.; Burns, P. L.; Holmes, A. B. Light-emitting diodes based on conjugated polymers. *Nature* **1990**, *347*, 539−541.

(5) Deng, X.-Y. Light-emitting devices with conjugated polymers. *Int. J. Mol. Sci.* **2011**, *12* (3), 1575−1594.

(6) Zhang, F.; Johansson, M.; Andersson, M. R.; Hummelen, J. C.; Inganäs, O. Polymer photovoltaic cells with conducting polymer anodes. *Adv. Mater.* **2002**, *14* (9), 662−665.

(7) Facchetti, A. π-Conjugated Polymers for Organic Electronics and Photovoltaic Cell Applications. *Chem. Mater.* **2011**, *23* (3), 733−758.

(8) Wang, K.; Wu, H.; Meng, Y.; Wei, Z. Conducting polymer nanowire arrays for high performance supercapacitors. *Small* **2014**, *10* (1), 14−31.

(9) Zhao, Z.; Richardson, G. F.; Meng, Q.; Zhu, S.; Kuan, H. C.; Ma, J. PEDOT-based composites as electrode materials for supercapacitors. *Nanotechnology* **2016**, *27* (4), 042001.

(10) Meng, Q.; Cai, K.; Chen, Y.; Chen, L. Research progress on conducting polymer based supercapacitor electrode materials. *Nano Energy* **2017**, *36*, 268−285.

(11) Guo, B.; Hu, Z.; An, Y.; An, N.; Jia, P.; Zhang, Y.; Yang, Y.; Li, Z. Nitrogen-doped heterostructure carbon functionalized by electroactive organic molecules for asymmetric supercapacitors with high energy density. *RSC Adv.* **2016**, *6* (46), 40602−40614.

(12) Russ, B.; Glaudell, A.; Urban, J. J.; Chabinyc, M. L.; Segalman, R. A. Organic thermoelectric materials for energy harvesting and temperature control. *Nat. Rev. Mater.* **2016**, *1*, 16050.

(13) Culebras, M.; Gómez, C. M.; Cantarero, A. Review on Polymers for Thermoelectric Applications. *Materials* **2014**, *7* (9), 6701−6732.

(14) MacDiarmid, A. G. "Synthetic Metals": A novel role for organic polymers. *Angew. Chem., Int. Ed.* **2001**, *40*, 2581−2590.

(15) Shakouri, A. Recent Developments in Semiconductor Thermoelectric Physics and Materials. *Annu. Rev. Mater. Res.* **2011**, *41* (1), 399−431.

(16) Chen, X.; Dai, W.; Wu, T.; Luo, W.; Yang, J.; Jiang, W.; Wang, L. Thin Film Thermoelectric Materials: Classification, Characterization, and Potential for Wearable Applications. *Coatings* **2018**, *8* (7), 244.

(17) Ates, M. A review on conducting polymer coatings for corrosion protection. *J. Adhes. Sci. Technol.* **2016**, *30* (14), 1510−1536.

(18) Joo, J.; Epstein, A. J. Electromagnetic radiation shielding by intrinsically conducting polymers. *Appl. Phys. Lett.* **1994**, *65* (18), 2278−2280.

(19) Makeiff, D. A.; Huber, T. Microwave absorption by polyaniline−carbon nanotube composites. *Synth. Met.* **2006**, *156* (7−8), 497−505.

(20) Partridge, A. C.; Harris, P.; Andrews, M. K. High sensitivity conducting polymer sensors. *Analyst* **1996**, *121*, 1349−1353.

(21) Sui, L.; Zhang, B.; Wang, J.; Cai, A. Polymerization of PEDOT/PSS/Chitosan-Coated Electrodes for Electrochemical Bio-Sensing. *Coatings* **2017**, *7* (7), 96.

(22) Kiefer, R.; Temmer, R.; Tamm, T.; Travas-Sejdic, J.; Kilmartin, P. A.; Aabloo, A. Conducting polymer actuators formed on MWCNT and PEDOT-PSS conductive coatings. *Synth. Met.* **2013**, *171*, 69−75.

(23) Nguyen, D. N.; Yoon, H. Recent Advances in Nanostructured Conducting Polymers: from Synthesis to Practical Applications. *Polymers* **2016**, *8* (4), 118.

(24) Heeger, A. J. Semiconducting and Metallic Polymers: The fourth generation of polymeric materials. *Angew. Chem., Int. Ed.* **2001**, *40*, 2591−2611.

DOI: 10.1021/acsaem.9b01985
ACS Appl. Energy Mater. 2020, 3, 861−867

(25) Culebras, M.; Gómez, C. M.; Cantarero, A. Enhanced thermoelectric performance of PEDOT with different counter-ions optimized by chemical reduction. *J. Mater. Chem. A* **2014**, *2* (26), 10109−10115.
(26) Bubnova, O.; Khan, Z. U.; Malti, A.; Braun, S.; Fahlman, M.; Berggren, M.; Crispin, X. Optimization of the thermoelectric figure of merit in the conducting polymer poly(3,4-ethylenedioxythiophene). *Nat. Mater.* **2011**, *10*, 429.
(27) Culebras, M.; Uriol, B.; Gómez, C. M.; Cantarero, A. Controlling the thermoelectric properties of polymers: application to PEDOT and polypyrrole. *Phys. Chem. Chem. Phys.* **2015**, *17* (23), 15140−15145.
(28) Xia, L.; Wei, Z.; Wan, M. Conducting polymer nanostructures and their application in biosensors. *J. Colloid Interface Sci.* **2010**, *341* (1), 1−11.
(29) Termentzidis, K. *Nanostructured Semiconductors: Amorphization and Thermal Properties*; Pan Stanford Publishing Pte. Ltd.: New York, 2017; p 574.
(30) Landfester, K. Miniemulsion polymerization and the structure of polymer and hybrid nanoparticles. *Angew. Chem., Int. Ed.* **2009**, *48* (25), 4488−507.
(31) Froimowicz, P.; Munoz-Espi, R.; Landfester, K.; Musyanovych, A.; Crespy, D. Surface-Functionalized Particles: From their Design and Synthesis to Materials Science and Bio-Applications. *Curr. Org. Chem.* **2013**, *17* (9), 900−912.
(32) Crespy, D.; Landfester, K. Miniemulsion polymerization as a versatile tool for the synthesis of functionalized polymers. *Beilstein J. Org. Chem.* **2010**, *6*, 1132−48.
(33) Culebras, M.; Serrano-Claumarchirant, J. F.; Sanchis, M. J.; Landfester, K.; Cantarero, A.; Gómez, C. M.; Muñoz-Espí, R. Conducting PEDOT Nanoparticles: Controlling Colloidal Stability and Electrical Properties. *J. Phys. Chem. C* **2018**, *122* (33), 19197−19203.
(34) Ran, F.; Tan, Y.; Dong, W.; Liu, Z.; Kong, L.; Kang, L. In situ polymerization and reduction to fabricate gold nanoparticle-incorporated polyaniline as supercapacitor electrode materials. *Polym. Adv. Technol.* **2018**, *29* (6), 1697−1705.
(35) Larrain, F. A.; Fuentes-Hernandez, C.; Chou, W.-F.; Rodriguez-Toro, V. A.; Huang, T.-Y.; Toney, M. F.; Kippelen, B. Stable solvent for solution-based electrical doping of semiconducting polymer films and its application to organic solar cells. *Energy Environ. Sci.* **2018**, *11* (8), 2216−2224.
(36) Culebras, M.; Choi, K.; Cho, C. Recent progress in flexible organic thermoelectrics. *Micromachines* **2018**, *9* (12), 638.
(37) Lu, Y.; Wang, J.-Y.; Pei, J. Strategies To Enhance the Conductivity of n-Type Polymer Thermoelectric Materials. *Chem. Mater.* **2019**, *31* (17), 6412−6423.
(38) Schlitz, R. A.; Brunetti, F. G.; Glaudell, A. M.; Miller, P. L.; Brady, M. A.; Takacs, C. J.; Hawker, C. J.; Chabinyc, M. L. Solubility-limited extrinsic n-type doping of a high electron mobility polymer for thermoelectric applications. *Adv. Mater.* **2014**, *26* (18), 2825−2830.
(39) Shi, K.; Zhang, F.; Di, C.-A.; Yan, T.-W.; Zou, Y.; Zhou, X.; Zhu, D.; Wang, J.-Y.; Pei, J. Toward high performance n-type thermoelectric materials by rational modification of BDPPV backbones. *J. Am. Chem. Soc.* **2015**, *137* (22), 6979−6982.
(40) Cho, C.; Culebras, M.; Wallace, K. L.; Song, Y.; Holder, K.; Hsu, J.-H.; Yu, C.; Grunlan, J. C. Stable n-type thermoelectric multilayer thin films with high power factor from carbonaceous nanofillers. *Nano Energy* **2016**, *28*, 426−432.
(41) Blackburn, J. L.; Ferguson, A. J.; Cho, C.; Grunlan, J. C. Thermoelectric Materials: Carbon-Nanotube-Based Thermoelectric Materials and Devices (Adv. Mater. 11/2018). *Adv. Mater.* **2018**, *30* (11), 1870072.
(42) Schneider, C. A.; Rasband, W. S.; Eliceiri, K. W. NIH Image to ImageJ: 25 years of image analysis. *Nat. Methods* **2012**, *9* (7), 671−675.
(43) van der Pauw, L. J. A method of measuring specific resistivity and Hall effect of discs of arbitrary shape. *Philips Res. Rep.* **1958**, *13*, 1−9.
(44) Liu, J.; Wang, X.; Li, D.; Coates, N. E.; Segalman, R. A.; Cahill, D. G. Thermal conductivity and elastic constants of PEDOT: PSS with high electrical conductivity. *Macromolecules* **2015**, *48* (3), 585−591.
(45) Zozoulenko, I.; Singh, A.; Singh, S. K.; Gueskine, V.; Crispin, X.; Berggren, M. Polarons, Bipolarons, And Absorption Spectroscopy of PEDOT. *ACS Applied Polymer Materials* **2019**, *1* (1), 83−94.
(46) Cho, C.; Bittner, N.; Choi, W.; Hsu, J. H.; Yu, C.; Grunlan, J. C. Thermally Enhanced n-Type Thermoelectric Behavior in Completely Organic Graphene Oxide-Based Thin Films. *Advanced Electronic Materials* **2019**, *5*, 1800465.
(47) Pan, L.; Hu, B.; Zhu, X.; Chen, X.; Shang, J.; Tan, H.; Xue, W.; Zhu, Y.; Liu, G.; Li, R.-W. Role of oxadiazole moiety in different D−A polyazothines and related resistive switching properties. *J. Mater. Chem. C* **2013**, *1* (30), 4556−4564.
(48) Pang, H.; Skabara, P. J.; Gordeyev, S.; McDouall, J. J.; Coles, S. J.; Hursthouse, M. B. Poly (3, 4-Ethylenediselena) thiophene the Selenium Equivalent of PEDOT. *Chem. Mater.* **2007**, *19* (2), 301−307.
(49) Lee, J.-K.; You, S.; Jeon, S.; Ryu, N.-H.; Park, K. H.; Myung-Hoon, K.; Kim, D. H.; Kim, S. H.; Schiff, E. A. Electron spin resonance and electrical transport in films of poly (3,4-ethylenedioxythiophene) doped with poly(styrenesulphonate). *J. Appl. Phys.* **2015**, *118* (1), 015501.
(50) Morris, J. D.; Wong, K. M.; Penaherrera, C. D.; Payne, C. K. Mechanism of the biomolecular synthesis of PEDOT:PSS: importance of heme degradation by hydrogen peroxide. *Biomater. Sci.* **2016**, *4* (2), 331−7.

DOI: 10.1021/acsaem.9b01985
ACS Appl. Energy Mater. 2020, 3, 861−867